



Electrochemical oxidation of sulfadiazine antibiotic using boron-doped diamond anode: application of response surface methodology for process optimization

Bahadır K. Körbahti*, Selin Taşyürek

Faculty of Engineering, Chemical Engineering Department, Mersin University, Çiftlikköy, 33343 Mersin, Turkey, Tel. +90 324 3610001, ext. 7374; Fax: +90 324 3610032; emails: korbahti@mersin.edu.tr, korbahti@gmail.com (B.K. Körbahti), selintasyurek@hotmail.com (S. Taşyürek)

Received 30 September 2014; Accepted 14 April 2015

ABSTRACT

Electrochemical oxidation and process optimization of sulfadiazine antibiotic were investigated in a batch electrochemical reactor using boron-doped diamond (BDD) anode. Reaction conditions were operated at 200–1,000 mg/L sulfadiazine concentration, 0–8 g/L supporting electrolyte (NaCl), 4–20 mA/cm² current density, and 25–45°C reaction temperature at 120 min reaction time. Process optimization was accomplished through response surface methodology in central composite designed experiments. Optimum operating conditions were determined under specified cost-driven constraints at 13.4 mA/cm² current density, 618 mg/L sulfadiazine concentration, 3.6 g/L electrolyte concentration, and 36°C reaction temperature. In a specific batch run at response surface-optimized conditions, the responses for sulfadiazine removal, COD removal, EOX, and energy consumption were achieved as 100.0%, 95.5%, 0.0617, and 94.3 kWh/kg COD_r, respectively. Relative error values in this optimization study for the electrochemical oxidation of sulfadiazine antibiotic using BDD anode were obtained below 2%.

Keywords: Boron-doped diamond; Electrochemical treatment; Optimization; Response surface methodology; Sulfadiazine

1. Introduction

Pharmaceuticals constitute a large group of human and veterinary medicinal compounds including antibiotics [1–5]. Antibiotics are chemotherapeutic agents that inhibit or abolish the growth of micro-organisms such as fungi, bacteria, or protozoa [1,2]. In the last years, the use of antibiotics in veterinary and human

medicine was widespread with an annual consumption of 100,000–200,000 tons [4]. However, increasing use of antibiotics and pharmaceuticals is dramatically causing environmental contamination throughout the world.

The residues of pharmaceuticals and antibiotics have been detected in aquatic environmental matrices, groundwater, surface water, drinking water, tap water, seawater, oceans, sediments and soil, and hospital wastewaters in lower and higher µg/L ranges

*Corresponding author.

[1–4]. This pollution was reported from hospital effluents, pharmaceuticals manufacturing processes, agricultural-influenced rivers, direct disposal of drugs in households and hospitals, excretion from urine or feces after drug administration to humans and animals, and WWTPs effluents [1,2,4,5].

Pharmaceutical wastewater from several matrices with insufficient treatment may leach into soil and then contaminate groundwater and surface water. As a result of contaminated water cycle, this contamination may affect drinking water treatment plants because most of the conventional wastewater treatment plants are not designed for removing pharmaceutical residuals from wastewater [4,6–8].

In order to prevent the contamination of water, several chemical, physical, physicochemical, biological, and advanced oxidation processes have been investigated. In recent years, advanced oxidation processes of UV/H₂O₂, ozonation, Fenton and photo-Fenton, semiconductor photocatalysis, sonolysis, wet air oxidation, and electrochemical oxidation were reported in the literature for the treatment of pharmaceuticals in water and wastewater [3,5,9].

Electrochemical processes are alternative methods for water and wastewater treatment due to disadvantages of the conventional methods such as high investment costs, discharge limitations, and large amounts of sludge [5,10]. In the literature, electrochemical oxidation of pharmaceuticals was investigated such as 17 β -estradiol, 17 α -ethinylestradiol, diclofenac, clofibrac acid, enrofloxacin, ibuprofen, ketoprofen, oxytetracycline hydrochloride, sulfamethoxazole, paracetamol, and tetracycline using Pt, Ti/RuO₂, Ti/SnO₂, Ti/IrO₂, Ti/RuO₂-IrO₂, and boron-doped diamond (BDD) electrodes [5,9].

In this study, electrochemical oxidation and process optimization of sulfadiazine (SDZ) antibiotic using BDD anode were investigated in a batch electrochemical reactor. Influence of operating variables of sulfadiazine concentration, electrolyte concentration, current density, and reaction temperature on sulfadiazine removal, COD removal, average quantification of electrochemical oxidation intermediates and byproducts (EOX), and energy consumption were investigated using response surface methodology (RSM). The main optimization objective was to determine optimum values of sulfadiazine concentration, electrolyte concentration, current density, and reaction temperature in order to achieve maximum sulfadiazine removal and COD removal with minimum EOX at minimized energy consumption.

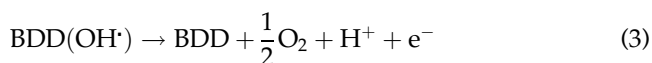
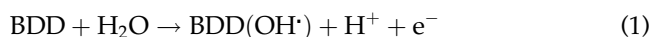
2. Theoretical background

2.1. Electrochemical process

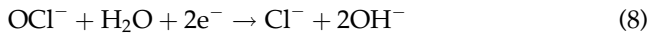
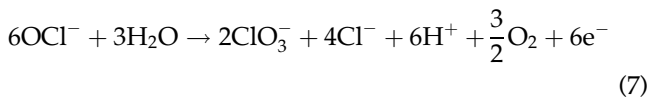
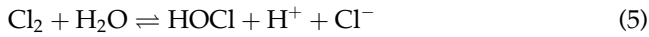
Direct and indirect oxidation mechanisms are responsible for the degradation of organic pollutants in electrochemical processes. Direct oxidation occurs at the anode surface and indirect oxidation occurs in the liquid bulk phase by the mediated oxidants [9–14].

BDD electrode is superior to the other electrodes such as Pt, TiO₂, IrO₂, PbO₂, SnO₂, and glassy carbon in electrochemical degradation processes due to its inert surface, good conductivity, corrosion resistance, significant chemical, electrochemical, and mechanical stability, and increased rates of mineralization with very high current efficiencies [15–18]. BDD anodes were used to treat organic pollutants in the literature such as cyanides, herbicides, organic acids, pharmaceuticals, cresols, naphthol, phenols, chlorophenols, nitrophenols, polyhydroxybenzenes, polyacrylates, surfactants, textile dyes, and real wastewaters [5,11,12].

Reaction mechanism at the BDD electrode is shown in Eqs. (1)–(3). In Reaction (1), BDD electrode produces weakly adsorbed hydroxyl radicals by the electrolysis of water discharge in the bulk phase. Hydroxyl radicals are not selective for the degradation of organic pollutants that they react with the organic pollutants (*R*), and mineralize them into CO₂ and H₂O. Reaction (2) is in competition with the side reaction of hydroxyl radical discharge to O₂ without any participation of the anode surface [10].



Indirect oxidation occurs in an undivided cell by the chlorine gas evolution at the anode when NaCl is used as a supporting electrolyte. Hydrolysis and ionization reactions occur rapidly when Cl₂ gas is dissolved in the aqueous phase [10,13,14,19–22], and then anodically generated OCl[−] and HOCl redox reagents can indirectly oxidize the organic pollutants. The distribution of OCl[−] and HOCl reagents in the aqueous phase depends on the solution pH [10,22,23]. Martínez-Huitle and Brillas [11] reported that trichloride ion (Cl^{3−}) is formed in very low concentration up to pH 4.0, while the predominant species is Cl₂ until pH near 3.0, HOCl in the pH range 3–8, and OCl[−] for pH > 8.0.



Indirect oxidation of sulfadiazine antibiotic resulted in sulfadiazine removal, COD reduction, and removal of intermediates and byproducts by *in situ* production of redox reagents of OCl^- and HOCl in the aqueous phase, and weakly adsorbed hydroxyl radicals produced at BDD anode in this study.

2.2. Design of experiments (DoE) and process optimization

RSM was used for the design of experiments (DoE) and process optimization. RSM is a mathematical and statistical method used for designing experiments, evaluating the influence of variables, searching optimum operating conditions, and building models in order to predict the targeted responses [24,25]. Central composite design (CCD) was used for DoE which is the most popular class of second-order designs. CCD with four independent variables at five levels was coded between the α values of -2 and $+2$ using Design-Expert 9.0 as outlined in Table 1. Four-factor designed experiments were augmented in two blocks with six replications at the design center in order to evaluate the pure error and were carried in randomized order. In the optimization process, the responses are related to chosen factors by linear or quadratic models. The quadratic model, which also includes the linear model, is given in Eq. (9) [24,25]:

$$\eta = \beta_0 + \sum_{i=1}^k \beta_i x_i + \sum_{i=1}^k \beta_{ii} x_i^2 + \sum_i \sum_{<j=2}^k \beta_{ij} x_i x_j \quad (9)$$

Experimental data were processed for Eq. (9) including ANOVA to obtain the interaction between the process variables and the responses. The quality of the fit of polynomial model was expressed by the coefficient of determination R^2 and R_{adj}^2 , and statistical significance was checked by F -values and P -values, and adequate precision ratio [22]. R^2 is a measure of the reduction amount in the variability of the response obtained by the independent factor variables in mathematical models. However, a large value of R^2 does not imply that the model fits very well to the experimental data. R^2 always increases with the addition of variables to the model whether the additional variable is statistically significant or not. R_{adj}^2 decreases as the number of terms in the model increases if those additional terms do not add value to the model. Therefore, it is possible to obtain mathematical models having large R^2 values that yield poor predictions of new observations or estimates of the response [24,25].

3. Materials and methods

3.1. Experimental setup and procedure

Stirred batch electrochemical reactor was made of DURAN[®] glass (Rettberg, Germany) having a reaction volume of 600 mL with heating/cooling jacket (Fig. 1). DIACHEM[®] boron-doped diamond (Nb/BDD) electrodes (CONDIAS, Germany) with an electrode surface area of 260 cm² were used as anode and cathode in a batch electrochemical reactor equipped with programmable Ametek Sorensen XFR 60-46 DC power supply, Heidolph RZR 2021 mechanical mixer, Lauda RE 630 S heating/cooling thermostat, and a Cole Parmer Masterflex[®] RZ-77924-60 peristaltic pump. Reaction started with the application of specified current density, and recycling water for temperature control was pumped through the reactor jacket. During electrochemical oxidation/degradation, 10 mL samples were withdrawn from the electrochemical reactor at predetermined time intervals for pH and conductivity measurements, and HPLC and COD analyses.

Table 1

Experimental design for the electrochemical oxidation of sulfadiazine antibiotic using BDD anode

Independent variables		Coded levels				
		-2	-1	0	+1	+2
x_1	Sulfadiazine concentration (mg/L)	200	400	600	800	1,000
x_2	NaCl concentration (g/L)	0	2	4	6	8
x_3	Current density (mA/cm ²)	4	8	12	16	20
x_4	Reaction temperature (°C)	25	30	35	40	45

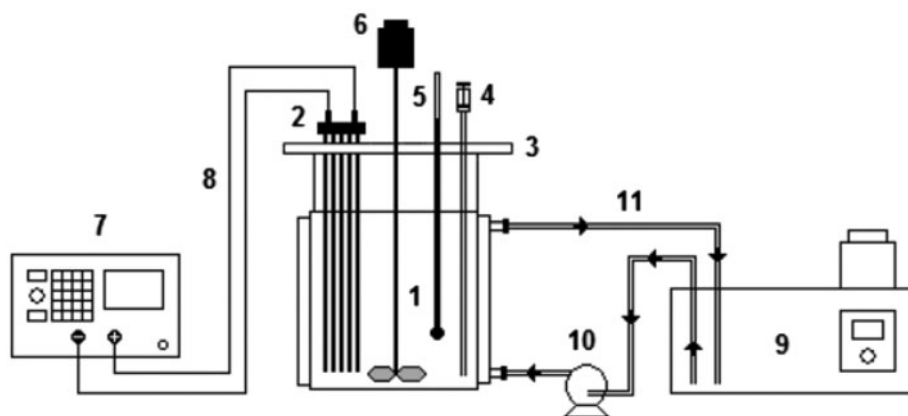


Fig. 1. Reactor system: (1) batch electrochemical reactor, (2) BDD electrodes, (3) Delrin[®] lid, (4) sampling cell, (5) thermometer, (6) mechanical mixer, (7) programmable DC power supply, (8) electrical connections, (9) heating/cooling thermostat, (10) peristaltic pump, and (11) heating/cooling feed.

3.2. Chemicals and materials

Sulfadiazine sodium salt (Fluka), sodium chloride (Merck), mercury sulfate (Merck), phosphoric acid (Merck), and acetonitrile (Merck) were purchased in extra pure grade and used as received. Molecular structure, chemical, and physical properties of sulfadiazine antibiotic are given in Table 2. GFL-2008 water still and Millipore Simplicity[®] UV ultrapure water system were used in our laboratory to produce double-distilled water (resistivity 18.2 MΩ cm@25°C, TOC < 5 ppb). COD concentrations were analyzed using Merck Spectroquant[®] 14541 COD cell tests.

3.3. Analysis

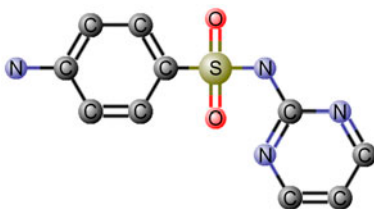
Analyses were done by the procedures outlined in standard methods for the examination of water and

wastewater [26]. High-performance liquid chromatography (HPLC) analysis was conducted using Inertsil ODS-3 (5 μm, 4.6 × 250 mm) column in a Shimadzu Prominence LC-20AD Liquid Chromatography equipped with SIL-20A auto sampler, CBM-20Alite System Controller, LC-20AD gradient pump, DGU-20A5 degasser, CTO-20A column oven, and SPD-20A UV/Vis detector. Binary solvent gradient (20:80) was used at a total flow rate of 1.5 mL/min with mobile phase A, acetonitrile with 0.01% phosphoric acid (v/v) and mobile phase B, water. Injection volume was constant at 5 μL. Column temperature was set at 35°C, and the detection of sulfadiazine antibiotic was set at 270 nm wavelength. pH and conductivity were measured using WTW inoLab BNC720 model pH meter/conductivity meter. COD analyses were done with 3 mL sample using Merck Spectroquant[®] 14541

Table 2

Molecular structure, chemical, and physical properties of sulfadiazine antibiotic

Molecular structure



Molecular formula

C₁₀H₉N₄NaO₂S

Synonyms

4-Amino-N-(2-pyrimidinyl)benzenesulfonamide sodium salt, SPS Agar Supplement

Molecular weight

272.26 g/mol

Water solubility

50 mg/mL H₂O

Appearance (Color)

Off-white

Solubility (Color)

Colorless to very faint yellow

CAS No.

547-32-0

COD cell tests. In order to prevent the interference in COD cell tests with Cl^- ions present in the sample, the samples were pretreated with required amounts of HgSO_4 prior to COD analysis according to COD correction procedures reported in the literature [27,28]. COD analyses were repeated twice for each sample and the results did not deviate more than $\pm 2\%$ in pair analyses.

4. Results and discussion

Experimental results were analyzed using approximating functions of $y_{\text{SDZ}\%}$, $y_{\text{COD}\%}$, y_{EOX} , and y_{EC} in Eqs. (10), (11), (13), and (15). x_1 , x_2 , x_3 , and x_4 are corresponding independent variables of sulfadiazine concentration (mg/L), electrolyte concentration (g/L), current density (mA/cm^2), and reaction temperature ($^\circ\text{C}$), respectively. ANOVA results of these quadratic models in Eqs. (10), (11), (13), and (15) are outlined in Table 3. Model F -values of 2.83, 8.45, and 66.09 indicate the models are significant for sulfadiazine removal, COD removal, and energy consumption, respectively; and F -value of 1.07 indicates the insignificance for EOX. Adequate precision measures the

signal-to-noise ratio and a ratio greater than four is desirable [22]. Therefore, in the quadratic models of sulfadiazine removal, COD removal, EOX, and energy consumption, the ratios of 9.743, 13.285, 4.660, and 33.913 indicate adequate signals for the models to be used to navigate the design space. P -values less than 0.0500 indicate the model terms are significant, whereas the values greater than 0.1000 are not significant [22]. In Table 3, the lack of fit F -values of 8.66, 5.17, and 8.69 indicate the significance for sulfadiazine removal, COD removal, and energy consumption, respectively; and F -value of 0.85 indicates the insignificance for EOX. Regression coefficients of R^2 and R^2_{adj} were well correlated with the actual and predicted values of sulfadiazine removal, COD removal, and energy consumption as outlined in Table 3. Quadratic models for the responses were well satisfied with the assumptions of the analysis of variance (ANOVA) according to normal probability, studentized residuals, and outlier- t residual plots (data not shown). Residual plots followed a normal distribution, and outlier- t values indicated that the approximations of the fitted models to the quadratic response surfaces were very good.

Table 3

ANOVA results of the quadratic models of sulfadiazine removal, COD removal, average quantification of intermediates and byproducts (EOX), and energy consumption

Source	SS	DF	MS	F -value	P -value
Sulfadiazine removal ^a					
Model	0.66	14	0.047	2.83	0.0142
Residual	0.37	22	0.017		
Lack of fit	0.35	17	0.021	8.66	0.0127
Pure error	0.012	5	2.400×10^{-3}		
COD removal ^b					
Model	1456.92	14	104.07	8.45	<0.0001
Residual	270.85	22	12.31		
Lack of fit	256.26	17	15.07	5.17	0.0392
Pure error	14.59	5	2.92		
EOX ^c					
Model	4.851×10^{-3}	14	3.465×10^{-4}	1.07	0.4302
Residual	7.119×10^{-3}	22	3.236×10^{-4}		
Lack of fit	5.295×10^{-3}	17	3.115×10^{-4}	0.85	0.6366
Pure error	1.824×10^{-3}	5	3.648×10^{-4}		
Energy consumption ^d					
Model	72595.75	14	5185.41	66.09	< 0.0001
Residual	1726.24	22	78.47		
Lack of fit	1669.70	17	98.22	8.69	0.0127
Pure error	56.53	5	11.31		

^a $R^2 = 0.6429$; $R^2_{\text{adj}} = 0.4156$; and adequate precision = 9.743.

^b $R^2 = 0.8432$; $R^2_{\text{adj}} = 0.7435$; and adequate precision = 13.285.

^c $R^2 = 0.4052$; $R^2_{\text{adj}} = 0.0268$; and adequate precision = 4.660.

^d $R^2 = 0.9768$; $R^2_{\text{adj}} = 0.9620$; and adequate precision = 33.913.

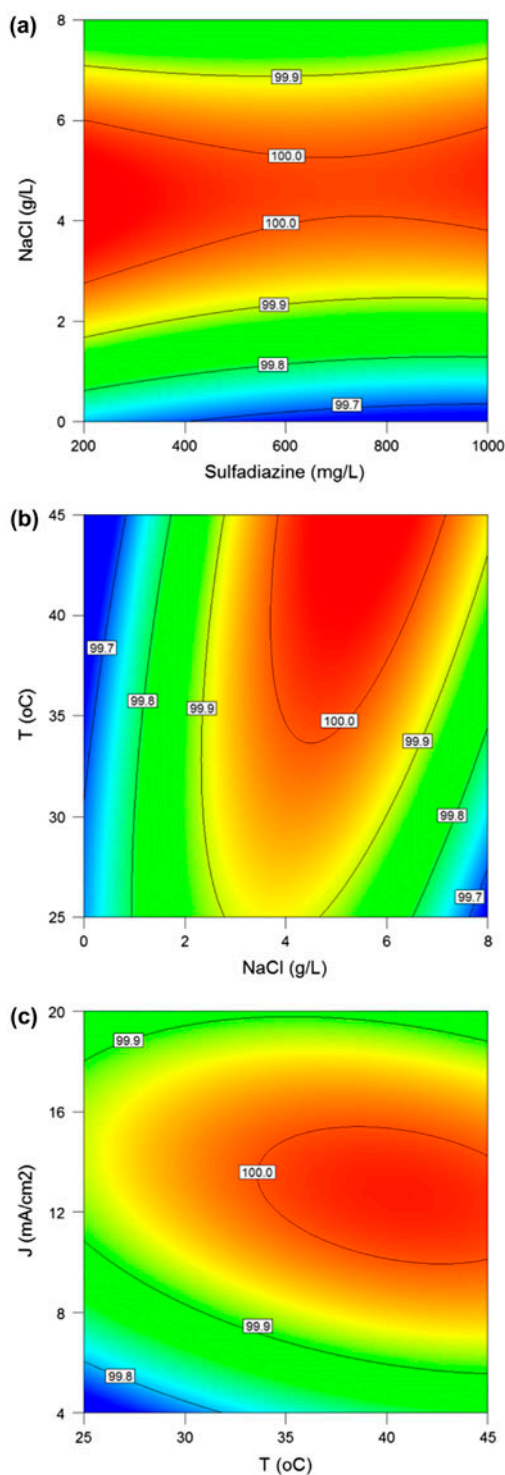


Fig. 2. Influences of independent variables on sulfadiazine (SDZ) removal: (a) influence of sulfadiazine concentration and electrolyte concentration (J : 12 mA/cm² and T : 35°C), (b) influence of electrolyte concentration and reaction temperature (SDZ: 600 mg/L and J : 12 mA/cm²), and (c) influence of reaction temperature and current density (SDZ: 600 mg/L and NaCl: 4 g/L).

Fig. 2(a)–(c) shows the influences of sulfadiazine concentration, electrolyte concentration, current density, and reaction temperature on sulfadiazine removal. Reaction conditions did not indicate a significant influence on sulfadiazine removal, whereas sulfadiazine removal was obtained between 99.0 and 100.0% with standard deviation 0.167% in this study. In Fig. 2, complete sulfadiazine removal was obtained in the region between 2.5 and 6.8 g/L NaCl and 5.6–19.8 mA/cm² current density between 200 and 1000 mg/L sulfadiazine concentration, and 25–45°C reaction temperature. Increase in electrolyte concentration increases the concentration of HOCl/OCl⁻ oxidizing reagents by anodic Cl₂ discharge in the reaction medium. However, electrolyte decomposition and gas evolution secondary reactions can also take place during the mineralization of organic pollutants that may result in a loss of current efficiency and a decrease in the removal yield [9,29]. Current density is the most important parameter for controlling the reaction rate in all electrochemical processes [22]. Although increase in current density increases electrochemical treatment efficiency, at very high cell voltages, most of the applied current is consumed by gas evolution and side reactions [9,30]. This phenomenon may cause a decrease in the current efficiency and a significant iR drop.

$$\begin{aligned}
 y_{SDZ} \% = & -1.97876 \times 10^{-4}x_1 + 0.13529x_2 + 0.086447x_3 \\
 & + 0.020383x_4 + 1.71875 \times 10^{-5}x_1x_2 + 1.48438 \\
 & \times 10^{-5}x_1x_3 - 6.87500 \times 10^{-6}x_1x_4 - 8.34132 \\
 & \times 10^{-3}x_2x_3 + 2.68750 \times 10^{-3}x_2x_4 - 4.06250 \\
 & \times 10^{-4}x_3x_4 + 1.26034 \times 10^{-7}x_1^2 - 0.015128x_2^2 \\
 & - 1.79453 \times 10^{-3}x_3^2 - 2.68933 \times 10^{-4}x_4^2 \\
 & + 98.82427
 \end{aligned} \tag{10}$$

In Fig. 3(a)–(c), the influences of sulfadiazine concentration, electrolyte concentration, current density, and reaction temperature on COD removal are shown. Increase in sulfadiazine concentration and decrease in NaCl electrolyte decreased COD removal yield. In Fig. 3(a), higher than 90% COD removal was achieved in the region above 3.3 g/L electrolyte concentration and below 678 mg/L sulfadiazine concentration. Electrolyte concentration had a positive effect on COD removal, and increase in NaCl concentration increased the COD removal efficiency by *in situ* production of HOCl/OCl⁻ redox reagents. In Fig. 3(b), higher than 90% COD removal was achieved in the region above 2.1 g/L electrolyte concentration and above 33°C reaction temperature. Process efficiency increased with

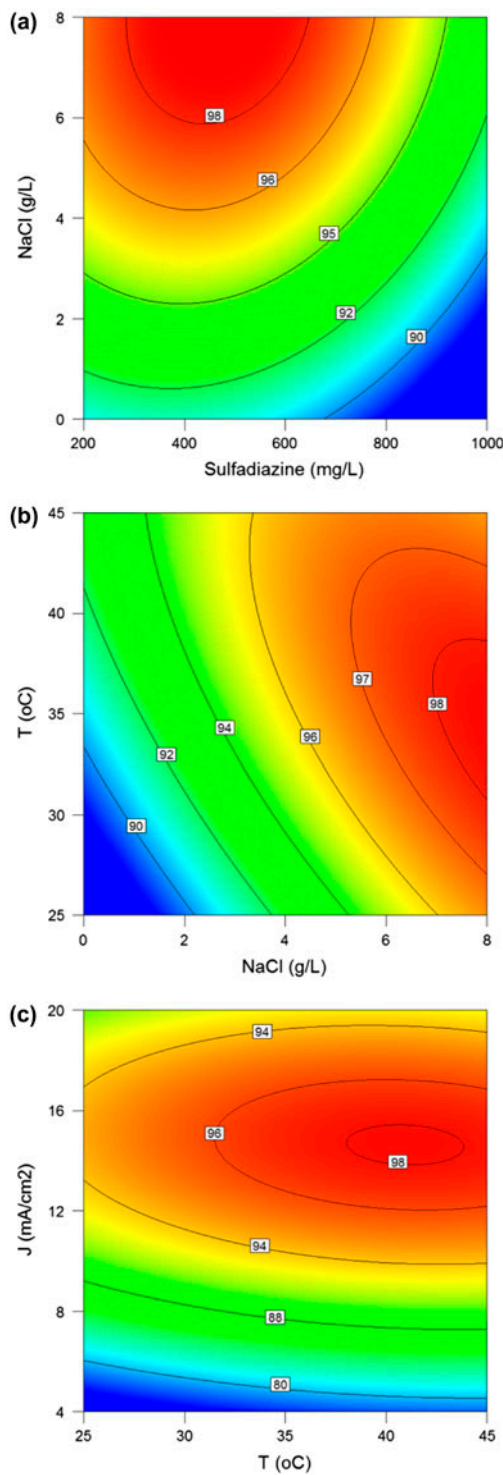


Fig. 3. Influences of independent variables on COD removal: (a) influence of sulfadiazine concentration and electrolyte concentration (J : 12 mA/cm² and T : 35°C), (b) influence of electrolyte concentration and reaction temperature (SDZ: 600 mg/L and J : 12 mA/cm²), and (c) influence of reaction temperature and current density (SDZ: 600 mg/L and NaCl: 4 g/L).

increase in current density due to *in situ* production of ·OH radicals at BDD anode and HOCl/OCl⁻ oxidizing reagents in the reaction medium. In Fig. 3(c), the reaction temperature did not indicate a significant influence on COD removal, and higher than 90% COD removal was obtained above 9.8 mA/cm² current density at all reaction temperatures.

In the literature, electrochemical oxidation of various organic pollutants was studied, and authors reported that increase in current density increased the removal of organic pollutants, COD removal, and energy consumption [17,31–35]. Comninellis and Chen [10] and Panizza and Cerisola [12] reported that for high organic concentrations or low current densities, COD decreases linearly due to local concentration of ·OH relative to organics concentration on the anode surface, which is affected independently by organic pollutant nature, current efficiency, and the amount of intermediates.

$$\begin{aligned}
 y_{\text{COD}} \% = & -0.044133x_1 + 3.51982x_2 + 3.80321x_3 \\
 & + 1.15275x_4 + 4.50000 \times 10^{-4}x_1x_2 + 3.27031 \\
 & \times 10^{-3}x_1x_3 + 5.05000 \times 10^{-4}x_1x_4 \\
 & - 0.022756x_2x_3 - 0.049125x_2x_4 - 0.010125x_3x_4 \\
 & - 1.76003 \times 10^{-5}x_1^2 - 0.10523x_2^2 - 0.17972x_3^2 \\
 & - 0.013572x_4^2 + 49.66815
 \end{aligned} \quad (11)$$

In this study, COD removal was obtained between 67.8 and 98.6% with standard deviation 6.92%. It is known that intermediates and reaction byproducts are produced in direct or indirect electrochemical oxidation processes before complete mineralization even in the absence of NaCl electrolyte [10]. Comninellis and Chen [10] indicated that the nature and amount of intermediates formed during electrochemical mineralization of organic compounds at BDD anodes depends on the process conditions. In the literature, it was reported that the main intermediates were aliphatic compounds such as oxalic and maleic acids which may undergo further anodic oxidation at a much lower rate [10,22,36,37]. Therefore, in our previous study [9], a novel parameter was defined in Eq. (12) for EOX from HPLC chromatograms by component mass balance and used in this study as well.

$$\text{EOX} = \frac{1}{\tau_R} \int_0^t \left(\frac{C(t)}{C_0} \right) dt \quad (12)$$

EOX number is always between 0 and 1, where EOX = 0 indicates mineralization without formation of

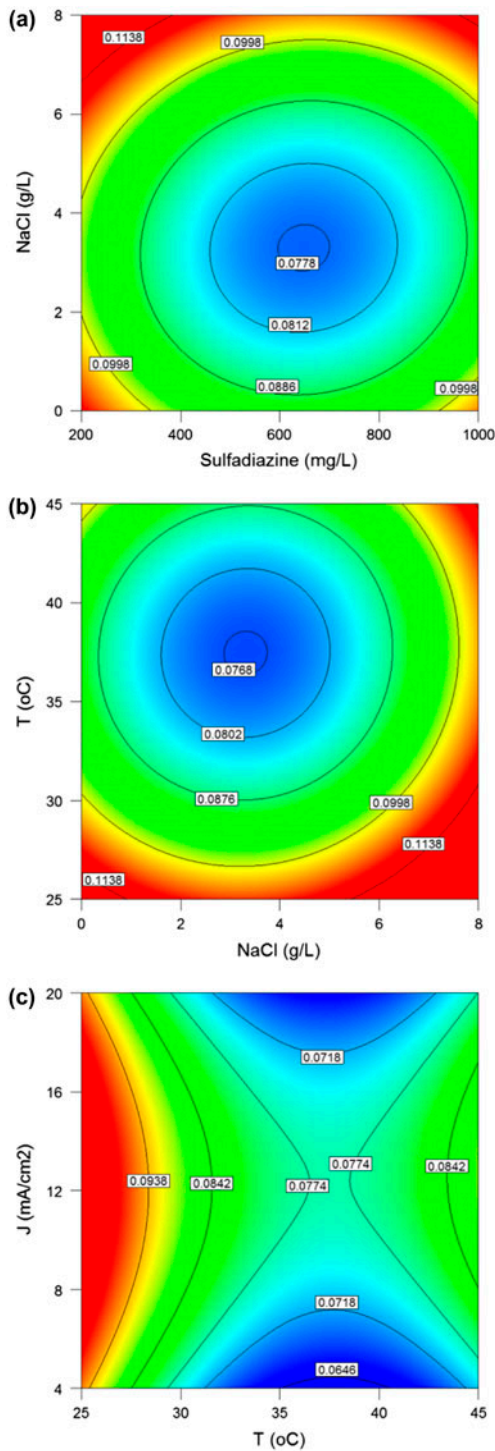


Fig. 4. Influences of independent variables on average quantification of electrochemical oxidation intermediates and byproducts (EOX): (a) influence of electrolyte concentration and sulfadiazine concentration (J : 12 mA/cm² and T : 35°C), (b) influence of electrolyte concentration and reaction temperature (SDZ: 600 mg/L and J : 12 mA/cm²), and (c) influence of reaction temperature and current density (SDZ: 600 mg/L and NaCl: 4 g/L).

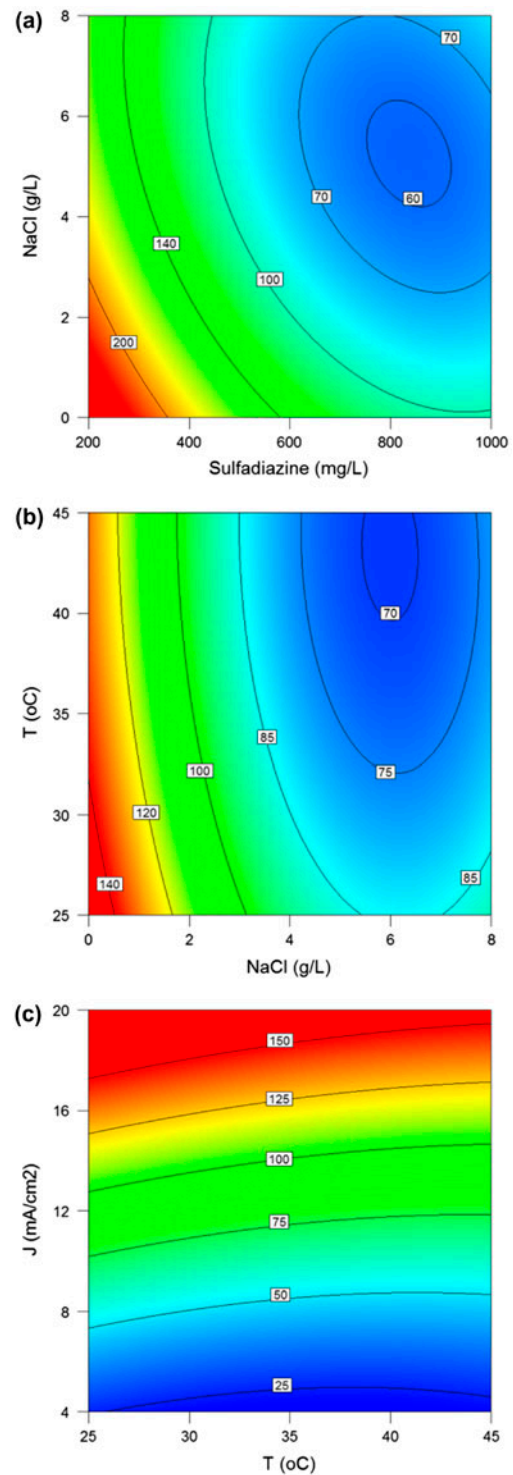


Fig. 5. Influences of independent variables on energy consumption: (a) influence of electrolyte concentration and sulfadiazine concentration (J : 12 mA/cm² and T : 35°C), (b) influence of electrolyte concentration and reaction temperature (SDZ: 600 mg/L and J : 12 mA/cm²), and (c) influence of reaction temperature and current density (SDZ: 600 mg/L and NaCl: 4 g/L).

intermediates and byproducts (complete combustion), and EOX = 1 indicates that organic compounds remained in the reaction medium as intermediates and byproducts without mineralization in the electrochemical oxidation process [9]. HPLC chromatograms showed that electrochemical degradation was rapid in first 10 min, while intermediates and byproducts began to form after two minutes. Intensity of the reaction intermediates reached a maximum at 30 min which was then oxidized during the electrolysis and completely disappeared in successive treatments.

Fig. 4(a)–(c) shows the influences of sulfadiazine concentration, electrolyte concentration, current density, and reaction temperature on EOX. EOX values were obtained between 0.0271 and 0.1048 with standard deviation 0.0181 in this study. The lowest EOX was found in the regions between 495 and 802 mg/L sulfadiazine concentration, 1.7–5.0 g/L electrolyte concentration, 10.2–14.6 mA/cm² current density, and 33–41 °C reaction temperature.

$$y_{\text{EOX}} = -1.07715 \times 10^{-4}x_1 + 1.70255 \times 10^{-3}x_2 + 7.65160 \times 10^{-3}x_3 - 0.014802x_4 - 1.07812 \times 10^{-6}x_1x_2 - 6.95312 \times 10^{-7}x_1x_3 - 3.81250 \times 10^{-7}x_1x_4 - 6.96720 \times 10^{-4}x_2x_3 - 2.68750 \times 10^{-5}x_2x_4 + 1.40625 \times 10^{-5}x_3x_4 + 1.02663 \times 10^{-7}x_1^2 + 1.25740 \times 10^{-3}x_2^2 - 2.01158 \times 10^{-4}x_3^2 + 1.99555 \times 10^{-4}x_4^2 + 0.33681 \quad (13)$$

Energy consumption values were calculated between 28.49 and 226.86 kWh/kg COD_r, with standard deviation 44.98 kWh/kg COD_r in the batch runs using Eq. (14).

$$E = \frac{iV_m\Delta t}{(COD_o - COD_t)V_R} \quad (14)$$

Fig. 5(a)–(c) shows the influences of sulfadiazine concentration, electrolyte concentration, current density, and reaction temperature on energy consumption. Energy consumption decreased with increase in sulfadiazine concentration and electrolyte concentration, while decrease in the current density. However, the reaction temperature was not found to be effective on energy consumption. In Fig. 5, energy consumption lower than 95 kWh/kg COD removed was obtained in the regions above 456 mg/L sulfadiazine concentration, above 3.4 g/L electrolyte concentration, and below 14.1 mA/cm² current density at all reaction temperatures. In this study, reasonable energy

consumption values were obtained according to the data previously reported in the literature [14].

$$y_{\text{EC}} = -0.30726x_1 - 22.18061x_2 + 20.87243x_3 - 3.25060x_4 + 0.012228x_1x_2 - 0.018859x_1x_3 + 1.46250 \times 10^{-4}x_1x_4 - 0.65462x_2x_3 + 0.045500x_2x_4 - 0.076187x_3x_4 + 2.77502 \times 10^{-4}x_1^2 + 1.73232x_2^2 + 0.20564x_3^2 + 0.044109x_4^2 + 165.17323 \quad (15)$$

In the study, efficiency maximization approach was preferred for the investigation of the optimum operating conditions. Optimum operating conditions were obtained at 618 mg/L sulfadiazine concentration, 3.6 g/L electrolyte concentration, 13.4 mA/cm² current density, and 36 °C reaction temperature as given in Table 4. In this study, the same optimum parameters were determined as in our previous study for electrochemical oxidation of ampicillin antibiotic using BDD

Table 4
Optimum operating conditions for the electrochemical oxidation of sulfadiazine antibiotic using BDD anode

Independent variables	Optimum RSM results
Sulfadiazine concentration (mg/L)	618
NaCl concentration (g/L)	3.6
Current density (mA/cm ²)	13.4
Reaction temperature (°C)	36

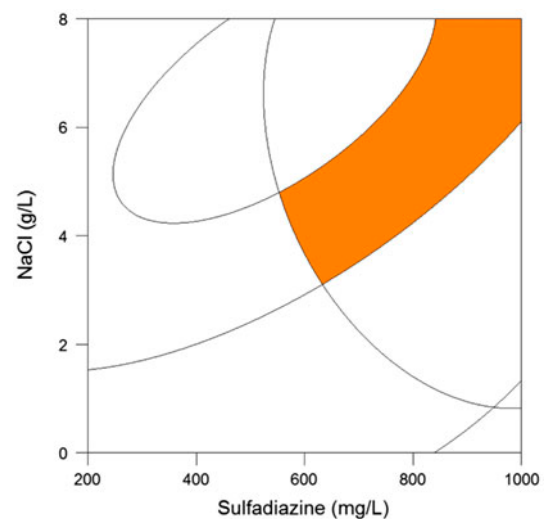


Fig. 6. Optimum operating region for the highest electrochemical oxidation efficiency of sulfadiazine antibiotic using BDD anode.

Table 5

Results of a specific batch run at response surface-optimized conditions for the electrochemical oxidation of sulfadiazine antibiotic using BDD anode

Response	Experimental result	RSM model	Error (%)
Sulfadiazine removal (%)	100.0	100.0	0.0
COD removal (%)	95.5	96.6	1.2
$EOX = \frac{1}{V_R} \int_0^t \left(\frac{C(t)}{C_0} \right) dt$	0.0617	0.0771	25.0
Energy consumption (kWh/kg COD _r)	94.3	92.5	1.9

anode [9]. This behavior could be attributed to the reaction kinetics and mass transfer limitations on the electrooxidation of pharmaceutical pollutants via *in situ* production of hydroxyl radicals at BDD anode and active chlorine in the reaction medium. Shaded region in Fig. 6 shows the efficiencies of higher than 99% sulfadiazine removal and higher than 90% COD removal between pH values 6.0 and 7.5, and below 95 kWh/kg COD_r energy consumption. The results of a specific batch run at response surface-optimized conditions are outlined in Table 5. Relative error values in this optimization study for the electrochemical oxidation of sulfadiazine antibiotic using BDD anode were obtained below 2% and indicated that the relationships developed between the responses and the independent variables were in very good agreement.

5. Conclusions

Electrochemical oxidation and process optimization of sulfadiazine (SDZ) antibiotic were investigated in a batch electrochemical reactor using BDD electrode. Based on experimental findings, an electrochemical system equipped with BDD electrode can be operated as a feasible and an effective oxidation and a detoxification stage for the treatment of pharmaceutical residues and hospital wastewater. In the study, electrolyte concentration and current density indicated positive influences on the removal efficiencies of sulfadiazine and COD due to *in situ* production of the redox reagents of OCl⁻ and HOCl in the aqueous phase, and weakly adsorbed hydroxyl radicals produced at BDD anode. However, the reaction temperature was not significant on sulfadiazine removal efficiency and energy consumption. In this study, a novel parameter was used for the determination of average quantification of electrochemical oxidation intermediates and byproducts (EOX) from HPLC chromatograms by component mass balance. Influence of operating parameters was analyzed using approximating functions of $y_{SDZ\%}$, $y_{COD\%}$, y_{EOX} , and y_{EC} , and optimum operating conditions were determined at 618 mg/L sulfadiazine concentration, 3.6 g/L electrolyte concen-

tration, 13.4 mA/cm² current density, and 36°C reaction temperature. Under response surface-optimized conditions, sulfadiazine removal, COD removal, EOX, and energy consumption were achieved as 100.0%, 95.5%, 0.0617, and 94.3 kWh/kg COD_r, respectively. In the optimization study, error values were obtained below 2% when the results of a specific batch run at optimum operating conditions compared with the approximate values of the response surface models. The results of this study indicated that the relationships developed between the responses and the independent variables were in very good agreement.

Acknowledgments

This project was supported by TÜBİTAK (The Scientific and Technological Research Council of Turkey) with grant number [111M341]. MSc dissertation was supported by Mersin University Scientific Research Projects Center (MEÜ BAP) with grant number [BAP-FBE KMB (ST) 2013-4 YL].

List of symbols

ANOVA	—	analysis of variance
BDD	—	boron-doped diamond
C ₀	—	total area of HPLC chromatogram at initial time ($t = 0$)
C(t)	—	area of HPLC chromatogram of intermediates and byproducts at time t
CCD	—	central composite design
COD	—	chemical oxygen demand (mg O ₂ /L, g O ₂ /L, mol O ₂ /L)
COD ₀	—	initial chemical oxygen demand (mg O ₂ /L, g O ₂ /L, mol O ₂ /L)
COD _r	—	COD removed
DF	—	degrees of freedom
DoE	—	design of experiments
E	—	energy consumption (kWh/kg COD _r)
EOX	—	average quantification of electrochemical oxidation intermediates and byproducts
J	—	current density (mA/cm ²)
k	—	number of independent variables (factors)

MS	—	mean square
R^2	—	coefficient of determination
R_{adj}^2	—	adjusted coefficient of determination
RSM	—	response surface methodology
SDZ	—	sulfadiazine
SS	—	sum of squares
t	—	reaction time (min, h)
T	—	reaction temperature (°C)
V_m	—	mean cell voltage (volt)
V_R	—	electrolyte volume or reaction volume (L, m ³)
x_i, x_j	—	independent variables (factors)
y	—	predicted value of the model (response)

Greek letters

$\beta_o, \beta_i, \beta_{ii}$	—	constant, linear, quadratic, and interaction coefficients in the approximation model
β_{ij}	—	
η	—	response
Δt	—	reaction time (min, h)
τ_R	—	total reaction time in stirred batch electrochemical reactor (min)

References

- [1] K. Kümmerer, Antibiotics in the aquatic environment—A review—Part I, *Chemosphere* 75 (2009) 417–434.
- [2] K. Kümmerer, Antibiotics in the aquatic environment—A review—Part II, *Chemosphere* 75 (2009) 435–441.
- [3] M. Klavarioti, D. Mantzavinos, D. Kassinos, Removal of residual pharmaceuticals from aqueous systems by advanced oxidation processes, *Environ. Int.* 35 (2009) 402–417.
- [4] V. Homem, L. Santos, Degradation and removal methods of antibiotics from aqueous matrices—A review, *J. Environ. Manage.* 92 (2011) 2304–2347.
- [5] I. Sirés, E. Brillas, Remediation of water pollution caused by pharmaceutical residues based on electrochemical separation and degradation technologies: A review, *Environ. Int.* 40 (2012) 212–229.
- [6] M.S. Díaz-Cruz, M.J. López de Alda, D. Barceló, Environmental behavior and analysis of veterinary and human drugs in soils, sediments and sludge, *TrAC, Trends Anal. Chem.* 22 (2003) 340–351.
- [7] N. Kemper, Veterinary antibiotics in the aquatic and terrestrial environment, *Ecol. Indic.* 8 (2008) 1–13.
- [8] M. Farré, S. Pérez, L. Kantiani, D. Barceló, Fate and toxicity of emerging pollutants, their metabolites and transformation products in the aquatic environment, *TrAC, Trends Anal. Chem.* 27 (2008) 991–1007.
- [9] B.K. Körbahti, S. Taşyürek, Electrochemical oxidation of ampicillin antibiotic at boron-doped diamond electrodes and process optimization using response surface methodology, *Environ. Sci. Pollut. Res.* 22 (2015) 3265–3278.
- [10] Ch. Comninellis, G. Chen (Eds.), *Electrochemistry for the Environment*, Springer, New York, NY, 2010.
- [11] C.A. Martínez-Huitle, E. Brillas, Decontamination of wastewaters containing synthetic organic dyes by electrochemical methods: A general review, *Appl. Catal., B* 87 (2009) 105–145.
- [12] M. Panizza, G. Cerisola, Direct and mediated anodic oxidation of organic pollutants, *Chem. Rev.* 109 (2009) 6541–6569.
- [13] B.K. Körbahti, K. Artut, Bilge water treatment in an upflow electrochemical reactor using Pt anode, *Sep. Sci. Technol.* 48 (2013) 2204–2216.
- [14] B.K. Körbahti, K. Artut, Electrochemical oil/water demulsification and purification of bilge water using Pt/Ir electrodes, *Desalination* 258 (2010) 219–228.
- [15] M. Panizza, G. Cerisola, Electrocatalytic materials for the electrochemical oxidation of synthetic dyes, *Appl. Catal., B* 75 (2007) 95–101.
- [16] X. Chen, G. Chen, F. Gao, P.L. Yue, High-performance Ti/BDD electrodes for pollutant oxidation, *Environ. Sci. Technol.* 37 (2004) 5021–5026.
- [17] E. Weiss, K. Groenen-Serrano, A. Savall, A comparison of electrochemical degradation of phenol on boron doped diamond and lead dioxide anodes, *J. Appl. Electrochem.* 38 (2008) 329–337.
- [18] Ch. Comninellis, A. Kapalka, S. Malato, S.A. Parsons, I. Poullos, D. Mantzavinos, Advanced oxidation processes for water treatment: Advances and trends for R&D, *J. Chem. Technol. Biotechnol.* 83 (2008) 769–776.
- [19] J.S. Do, W.C. Yeh, Paired electrooxidative degradation of phenol with *in situ* electrogenerated hydrogen peroxide and hypochlorite, *J. Appl. Electrochem.* 26 (1996) 673–678.
- [20] S.H. Lin, C.T. Shyu, M.C. Sun, Saline wastewater treatment by electrochemical method, *Water Res.* 32 (1998) 1059–1066.
- [21] C.J. Israilides, A.G. Vlyssides, V.N. Mourafeti, G. Karvouni, Olive oil wastewater treatment with the use of an electrolysis system, *Bioresour. Technol.* 61 (1997) 163–170.
- [22] B.K. Körbahti, Response surface optimization of electrochemical treatment of textile dye wastewater, *J. Hazard. Mater.* 145 (2007) 277–286.
- [23] G. Tchobanoglous, F.L. Burton, H.D. Stensel (Eds.), *Wastewater Engineering, Treatment and Reuse*, McGraw-Hill, New York, 2004.
- [24] D.C. Montgomery, *Design and Analysis of Experiments*, John Wiley & Sons, New Jersey, NJ, 2009.
- [25] R.H. Myers, D.C. Montgomery, C.M. Andersen-Cook, *Response Surface Methodology: Process and Product Optimization using Designed Experiments*, John Wiley & Sons, New Jersey, NJ, 2009.
- [26] American Public Health Association (APHA), *Standard Methods for the Examination of Water and Wastewater*, Maryland, 1999.
- [27] E.R. Burns, C. Marshall, Correction for chloride interference in the chemical oxygen demand test, *Water Environ. Res.* 37 (1965) 1716–1721.
- [28] F.J. Baumann, Dichromate reflux chemical oxygen demand. Proposed method for chloride correction in highly saline wastes, *Anal. Chem.* 46 (1974) 1336–1338.
- [29] A. Fernandes, A. Morão, A. Magrinho, A. Lopes, I. Gonçalves, Electrochemical degradation of C.I. Acid Orange 7, *Dyes Pigment.* 61 (2004) 287–296.
- [30] Z.M. Shen, D. Wu, J. Yang, T. Yuan, W.H. Wang, J.P. Jia, Methods to improve electrochemical treatment effect of dye wastewater, *J. Hazard. Mater.* 131 (2006) 90–97.

- [31] R. Bellagamba, P. Michaud, Ch. Comninellis, N. Vatistas, Electro-combustion of polyacrylates with boron-doped diamond anodes, *Electrochem. Commun.* 4 (2002) 171–176.
- [32] E. Weiss, K. Groenen-Serrano, A. Savall, Electrochemical degradation of sodium dodecylbenzene sulfonate on boron doped diamond and lead dioxide anodes, *J. New Mater. Electrochem. Syst.* 9 (2006) 249–256.
- [33] B. Louhichi, M.F. Ahmadi, N. Bensalah, A. Gadri, M.A. Rodrigo, Electrochemical degradation of an anionic surfactant on boron-doped diamond anodes, *J. Hazard. Mater.* 158 (2008) 430–437.
- [34] M. Panizza, M. Delucchi, G. Cerisola, Electrochemical degradation of anionic surfactants, *J. Appl. Electrochem.* 35 (2005) 357–361.
- [35] T. González, J.R. Domínguez, P. Palo, J. Sánchez-Martín, E.M. Cuerda-Correa, Development and optimization of the BDD-electrochemical oxidation of the antibiotic trimethoprim in aqueous solution, *Desalination* 280 (2011) 197–202.
- [36] J. Naumczyk, L. Szpyrkowicz, F. Ziliograndi, Electrochemical treatment of textile wastewater, *Water Sci. Technol.* 34 (1996) 17–24.
- [37] C.A. Martínez-Huitle, L.S. Andrade, Electrocatalysis in wastewater treatment: recent mechanism advances, *Quim. Nova* 34 (2011) 850–858.